



Prognostic analysis of adhesively bonded lap joints with cracks in adherents

I. Syed¹ · L. Chikmath² · M. N. Ramanath² · H. Murthy² · B. Dattaguru¹

Received: 25 March 2020 / Revised: 27 April 2020 / Accepted: 4 May 2020 / Published online: 12 May 2020
© Institute of Smart Structures & Systems, Department of Aerospace Engineering, Indian Institute of Science, Bangalore 2020

Abstract

The strength of adhesively bonded joints is a primary concern when crack like damages initiates in the adherent/adhesive and tends to grow during their service life. In addition to the extent of damage, its position affects the strength and remaining fatigue life of these joints. Prognosis approach to estimate the remaining life of these joints in the presence of damage in adherent plates at any stage of operational fatigue loading is presented in this paper. Three-dimensional finite-element material and geometric nonlinear analysis is carried out. These joints are analysed for peel and shear stresses when subjected to axial loading, and failure load is estimated using an average stress criterion over a characteristic distance. Crack growth studies are carried out by introducing the crack in the adherent plates at different locations. Fracture parameters are computed by employing modified virtual crack closure integral, and crack growth is modelled using Paris law with Elber correction. The results obtained are of significance to structural health monitoring applications of these adhesively bonded joints which assist in scheduling the maintenance operations.

Keywords Adhesively bonded joints · Failure load · Crack · Prognosis

List of symbols

a	Crack length
a_0 and a_c	Initial and critical crack lengths
a' and b'	Material constants in Elber's crack growth model
C and m	Material constants in Paris law
E and ν	Young's modulus and Poisson's ratio
G_I	Mode I strain energy release rate (SERR)
K_I	Mode I stress intensity factor (SIF)
K_{eff} and K_{IC}	Effective SIF and mode I fracture toughness
K_{max} and K_{min}	Maximum and minimum SIF
N	Number of cycles to failure
P_f	Failure load
R and R_p	Stress ratio = $\frac{\sigma_{\text{min}}}{\sigma_{\text{max}}}$ and load ratio = $\frac{P_{\text{min}}}{P_{\text{max}}}$

U and θ	Translational and rotational displacements
σ_{vm} and σ_y	von Mises and yield stress

Introduction

Generally, the structural systems in aerospace vehicles are made in modules and joints play an important role in connecting them (Shanley 1943; Vivek 2007). Several regions of high stress concentrations are developed in riveted/fastener joints due to their geometric irregularities, which consequently lead to stress singularities with usage that turn out to be potential crack initiation locations. Unlike these joints, adhesively bonded joints offer smooth cascade of load transfer with relatively lesser high stress locations due to their geometry and configuration (Mortensen and Thomsen 2002). Figure 1 shows the typical configuration of a single lap joint where the adherent plates are joined by a thin film of adhesive and the load flow path when subjected to axial loading.

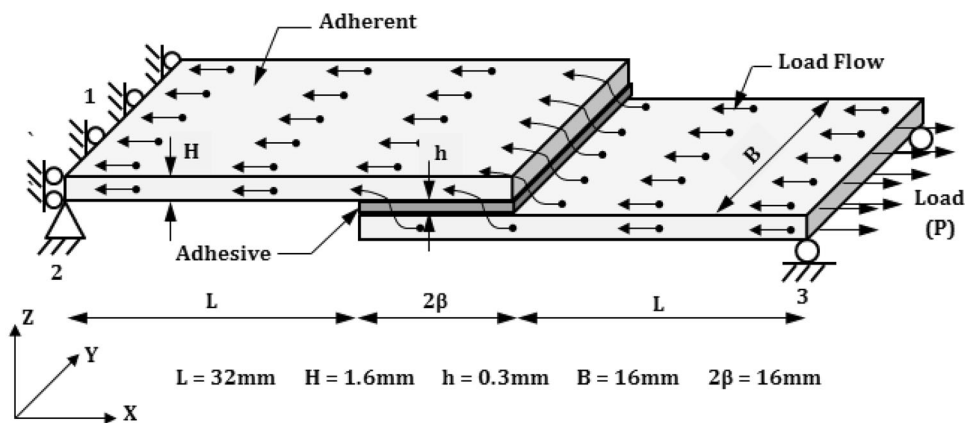
In addition, it is noticed that the adhesively bonded joints offer better ductility, higher peel and shear stresses resulting in higher static strength (Hart-Smith 1973). Subsequently, this results in better fatigue life of adhesively

✉ L. Chikmath
lokamanyachikmath@gmail.com

¹ Department of Aerospace Engineering, Jain (Deemed-to-be-University), Bengaluru 562112, India

² Department of Aerospace Engineering, Indian Institute of Technology-Madras, Chennai 600036, India

Fig. 1 Load flow in adhesively bonded joints



bonded joints (Kinloch and Osiyemi 1993). Further, from manufacturing perspective, the complexity in assembly process of these joints is relatively uncomplicated compared to fastener joints. These advantages of adhesively bonded joints offer immense potential in many applications of several engineering components, especially in aircraft structures where the weight is of prime concern.

One of the issues limiting the wide-scale application of adhesively bonded joints is the lack of understanding of their durability or long-term behaviour (Sargent 2005). Several studies have been carried out in the past decades on the strength of these joints based on de-bond and de-bond growth and correlated with fracture parameters in the mid-bond line of the adhesives (Adams and Peppiatt 1974; Philip et al. 2006; Sahoo et al. 2012). However, the failure studies of these joints in the presence of crack-like damages in adherent plates are sporadic. Hitherto, few researchers have studied the behaviour of adhesively bonded joints with defects like cutout section in the adherents and by introducing artificial damages (Karachalios et al. 2013; Jamal-Omidi and Mohammadi 2018). Besides, the literature covering various aspects of cracks and their position in the adherent plates which would affect the strength of these joints is scanty. The aforementioned issues are addressed in this paper wherein the remaining life of these joints is estimated in the presence of the cracks in adherent plates at various locations by utilizing well-established models/techniques by prognostic approach. The approach adopted and the data generated through the study would enable better damage-tolerant design of these joints and would assist in better assessment of their health (Bharath and Chikmath 2017).

Problem definition

The geometry and configuration of the adhesively bonded single lap joint analysed in this paper are shown in Fig. 1 of Sect. 1 which is taken from the literature (Pandey and

Narasimhan 2001). Here, ' L ' is the length of the adherent plates till the bond region, ' B ' is the width of the adherent plates, ' 2β ' is the length of the adhesive on which the adherent plates are bonded together (overlap region), ' H ' and ' h ' are the thicknesses of adherent plates and adhesive, respectively. One end of the lap joint is supported on the rollers, and the other is subjected to in-plane loading (P). FM 73 is taken as the adhesive to bond the two 4340 alloy steel adherents. In later stages, the adherent material is changed from 4340 alloy steel to aluminium alloy (Al2024-T3) for parametric study. The material properties considered in the analysis are listed in Table 1.

Methodology

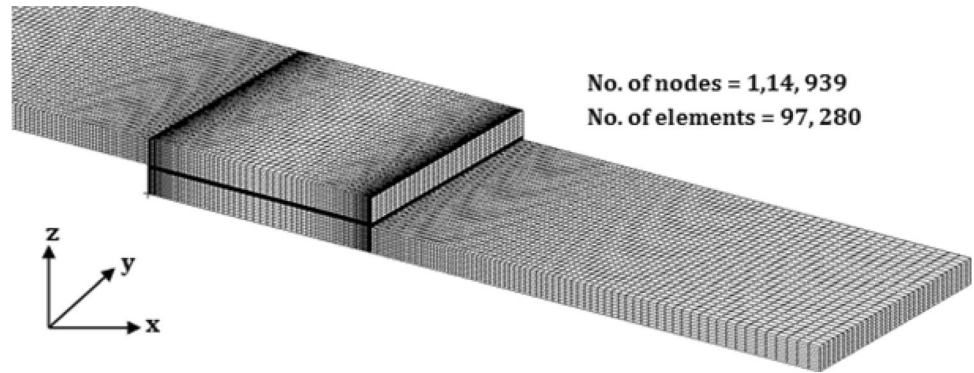
FE modelling

Numerical study of single lap joints is carried out using three-dimensional finite-element analyses (FEA) with eight-node brick elements and post-processed in MSC PATRAN (2017). The effect of geometric and material nonlinearity is studied using MSC NASTRAN (2017) FEA tool. Adherents and adhesive are assumed to be homogeneous and isotropic, and perfect bonding between them exists (i.e. no de-bonding). Adhesive is considered to be elastic/perfectly plastic (Young's modulus of 2.2 GPa, yield strength of 40.0 MPa). The FE model of the above configuration is shown in Fig. 2. From the convergence study with respect to peel stress, the number of nodes and that of elements are frozen to be 114,939 and 97,280, respectively, for further analysis. The necessary boundary conditions of the configuration in Fig. 1 are given below (Eqs. 1–3). The bottom adherent is subjected to axial load (P) in positive x -direction, while the top adherent is supported by rollers.

Table 1 Material properties (Pandey and Narasimhan 2001; Gomez et al. 1976) of constituents in adhesively bonded joints

Properties	Adherent (4340 alloy steel)	Adherent (Al 2024-T3)	Adhesive (FM 73)
E	210 GPa	72 GPa	2.2 GPa
ν	0.33	0.3	0.43
σ_{yield}	523 MPa	324 MPa	40 MPa
K_{IC}	1582 MPa $\sqrt{\text{mm}}$	790 MPa $\sqrt{\text{mm}}$	–

Fig. 2 Three-dimensional FE model of adhesively bonded joint



On the adherent with support condition (1) :

$$U_x = 0 \quad U_z = 0 \quad \theta_z = 0 \tag{1}$$

Rigid body motion constraint (2) : $U_y = 0$ (2)

On the loading edge of the adherent (3) : $U_z = 0 \quad \theta_z = 0$ (3)

Geometric and material nonlinear analysis

The predominant concern in the analysis of single lap joint is the eccentricity of the load path between adherent plates causing geometric nonlinearity, which leads to large deformations in addition to bending action (Hart-Smith 1973). Hence, geometric nonlinear analysis is performed in NASTRAN software. Such an analysis reduces the deflections, leading to stiffer structure (Dattaguru et al. 1984). Further, due to the nature of the problem, the characteristic material property, especially that of adhesive, which is elastic/perfectly plastic (Fig. 3) plays a key role during computation of the failure load. Because adhesive has low yield strength, the material nonlinearity would cause noticeable stress distribution along the mid-bond line of it. This material nonlinearity essentially reduces the peak stresses in the bond region.

Estimation of failure load (P_f)

Failure load estimation in adhesively bonded joints is severely affected by the extremely low yield strength and plastic deformation in the adhesives (Chun and Peter

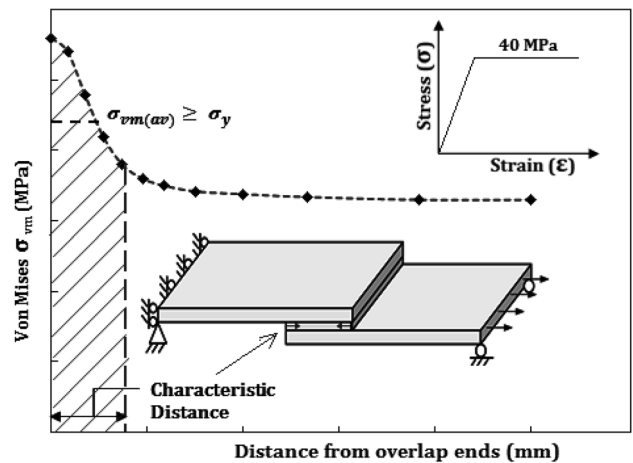


Fig. 3 Characteristic distance for estimation of failure load by average stress criterion

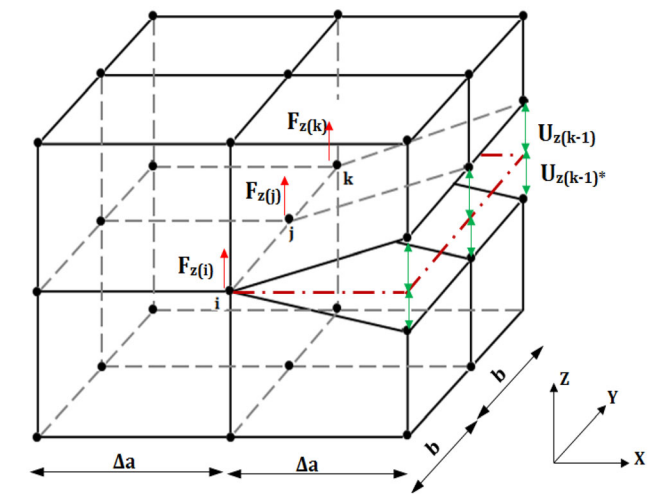
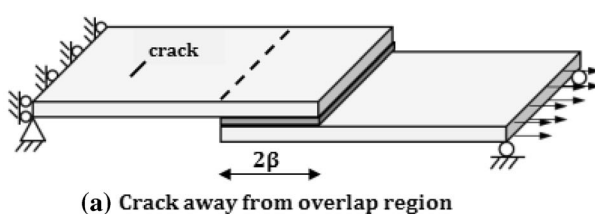
2000). Hence, failure analysis of this single-lap joint becomes substantial to the design of aerospace vehicles. Due to the presence of elastic singularities at the ends of the overlap region, the load causing the failure of the adhesively bonded joint is estimated using average stress criterion (Clark and McGregor 1993). Prior to this, the stress variation along the mid-bond line of the adhesive region is studied wherein the peel and shear stresses play a significant role in understanding the load transfer phenomenon (Hart-Smith 1973). Several researchers (Tsai and Morton 1994) have demonstrated experimentally and analytically the criterion to estimate the failure load of adhesively bonded joints which find their application during

material nonlinear analysis. Among them, characteristic distance in the overlap region becomes a critical parameter, since the stresses will be in a singular state at the ends of the overlap region (Kumar et al. 2018). Estimating the failure load over the characteristic distance using average stress criterion is shown in Fig. 3. The stresses are averaged over the characteristic distance and correlated with the yield strength to ascertain failure. In the current analysis, this characteristic distance is 2.7% of overlap length taken from the overlap end, which is experimentally proven to be good in predicting failure load (Gopalan 1991).

Damage growth studies in adherent plates

Many structural components of aircraft are designed based on damage tolerance design concept in which damage such as a crack that cannot be detected through NDT with 95% probability is assumed to be present (Haapalainen and Leskela 2012). The size of this crack is much smaller than the critical crack size, which could cause fracture. However, with usage, this damage could grow and reach a critical stage causing adverse effects that can lead to failure of the structure. Such cracks that could grow in the adherent plates during the service life of the structure are analysed. Initial crack length of $(\frac{a_0}{B} = 0.0625)$ is assumed in the adherent, and the effect of crack location on the crack growth life is studied by introducing crack within and away from the overlap regions as shown in Fig. 4. The crack growth analysis is conducted where maximum load in the fatigue cycles is taken to be 75% of the failure load of these joints (Struck 1977).

Mode I fracture analysis is performed for these damages in adherent plates. It is verified that there is no significant contribution from the other two modes (mode II and mode III) towards the crack growth. MVCCI technique is used in estimating fracture parameters during the crack growth studies as given in Eqs. 4 and 5, respectively (Badari Narayana et al. 1994) and is pictorially explained in Fig. 5 for an eight-node brick element. Crack growth life is estimated by Paris law with Elber correction as given in Eq. 6 (Elber 1971) with the necessary constants in the equation taken from the literature (Gomez et al. 1976).



(a) Crack away from overlap region

Fig. 5 MVCCI formulation to compute fracture parameters

$$G_I = \frac{1}{2\Delta A} \left[F_{z(k)} \left(U_{z(k-1)} + U_{z(k-1)^*} \right) + F_{z(j)} \left(U_{z(j-1)} + U_{z(j-1)^*} \right) \right] \tag{4}$$

$$K_I = \sqrt{G_I E} \tag{5}$$

where $\Delta A = \Delta a^* b$, Δa = element length at crack front, b = width of the element.

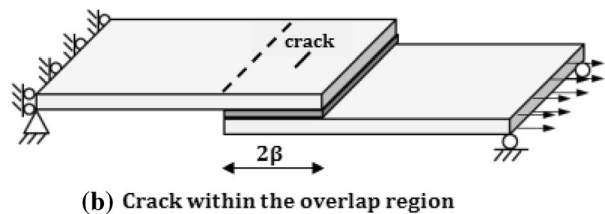
$$\frac{da}{dN} = C(\Delta K_{eff})^m \quad \text{with} \quad \Delta K_{eff} = K_{max} - K_{min} \tag{6}$$

where $K_{min} = (a' + b'R)K_{max}$ and $K_{max} = \sigma_{max} \sqrt{\pi a_c}$.

Results and discussions

Shear and peel stresses

The finite element analysis is conducted with the material properties given in Table 1 and the mesh shown in Fig. 2. The shear and peel stresses computed in the mid-bond region of the adhesive that induce failure of the joint are shown in Figs. 6 and 7, respectively. The shear stress and peel stress distributions in the mid-bond region are nearly symmetric. The marginal disturbance in their symmetry could be due to the imposed boundary conditions at the two ends. Both the stresses are higher at ends of the overlap region and are



(b) Crack within the overlap region

Fig. 4 Damage in adherent plates

Fig. 6 Shear stress variation along the bond region

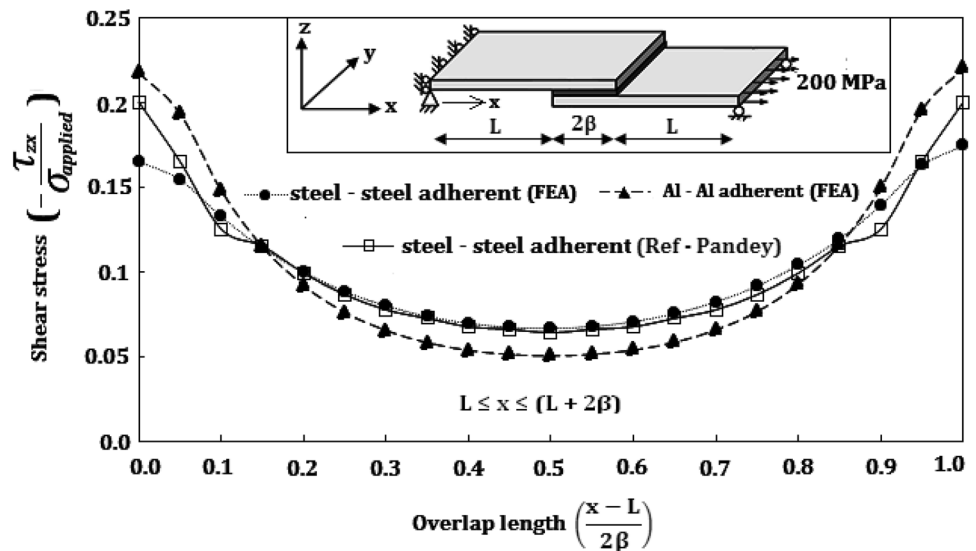
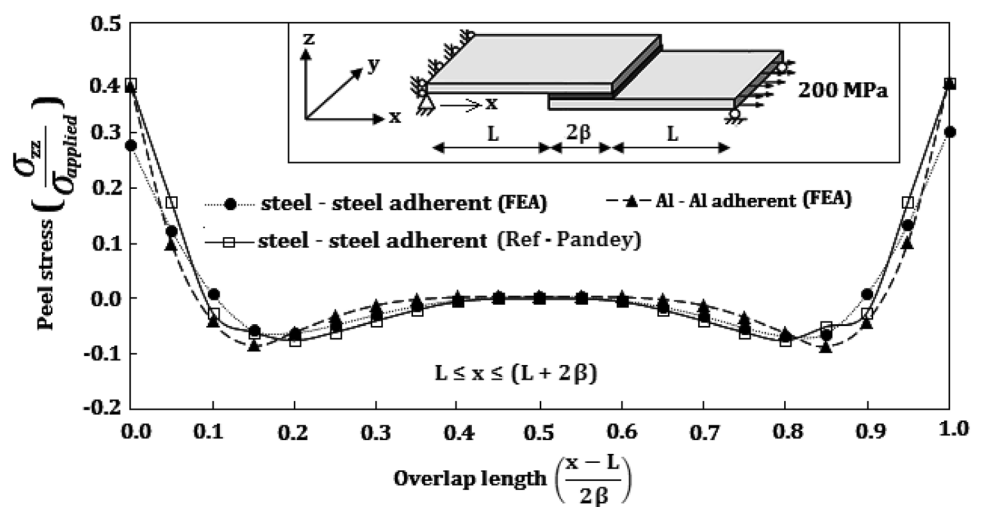


Fig. 7 Peel stress variation along the bond region



lower towards the centre. Ends possess higher stresses due to the eccentric loading path and due to the presence of discontinuities. For validation, results of current FEA are compared with those from the literature (Pandey and Narasimhan 2001). They match very well for steel–steel adherent, and the minor differences seen are due to possible slight variations in the FEM mesh and the difference in nature of the elements used (20-noded elements were used in the quoted reference). As a parametric variation, the adherent material is taken as aluminium plate instead of 4340 alloy steel. Only marginal differences were noticed in both the shear and peel stresses between Al–Al and steel–steel adherents since the adhesive remains the same.

Failure load

Average von Mises stress over the characteristic distance is used to estimate the failure load of adhesively bonded joint

as discussed in Sect. 3.3. The applied load that causes the average von Mises stress to be equal to or greater than the yield strength of the adhesive is considered to be load causing the failure of the joint. This failure load is arrived at after several iterations of load applied. The failure loads computed for adhesively bonded joints with different adherent materials are shown in Table 2. The variation in failure load from Al–Al adherent combination to steel–steel combination is not significant, while the adhesive is the same. Hence, for further analysis of crack growth, Al–Al adherent is considered since crack propagation rate is relatively faster in them compared to steel adherent plates.

Crack growth analysis

Crack growth analysis is carried out with two overlapping aluminium adherent plates joined together using adhesive FM 73 to form an adhesively bonded lap joint. For the

Table 2 Failure loads of adhesively bonded joint for different adherent plates

Adherent plate combination	Average von Mises stress (MPa)	Failure load (P_f) (MPa)
Al–Al	40.08	260
Steel–steel	40.02	265

σ_y of adhesive = 40 MPa and characteristic distance is 2.7% of the lap length

applied load (P), the variations in the SIF along the depth of the crack measured along the thickness from top to bottom (z -direction) are shown in Fig. 8, for two different crack locations: (a) away from the overlap region and (b) in the overlap region. In both the cases, the crack is located only in the adherent plates. SIF varies significantly when measured from top to bottom depthwise for crack at location (a). This may be the result of bending of the adherent due to the applied load. In contrast, there is only marginal depthwise reduction in SIF when the crack is at location (b). This is due to lesser bending of the adherents and also the presence of adhesive in the overlap region which tries to resist the crack growth depthwise. Further, the overlap region is relatively stiffer than the nonoverlap region and the presence of adhesive can retard further crack growth, thereby reducing the SIF as compared to the earlier case.

Considering the maximum depthwise SIF variation in the adherent plates away from the overlap region, SIF is computed for crack at different locations away from the overlap regions and is shown in Fig. 9. It is observed that the SIF for same crack size increases as the distance (λ/L) of location of the crack increases from the support ends. The SIF for every crack length at the location away from the support conditions ($\lambda/L = 0.875$) is nearly more than twice the value of SIF near the supports ($\lambda/L = 0.125$). This is because the crack that is farther from the support conditions experiences higher bending effects than the cracks that are near the support conditions and are closer to the

discontinuities of the lap region, which is indicated in Fig. 10 with deformed shape of the lap joint. Further, when the crack is at the distance $\lambda/L = 1$, i.e. at the start of the overlap region, crack propagation along the depthwise direction experiences the mode II fracture failure (in-plane shear) and the values of SIF are too low when compared with cracks at other locations.

Further crack growth studies are conducted for the cracks that are located at critical locations in the adherents ($\lambda/L = 0.625, 0.75, 0.875$) away from the overlap region which is identified from the previous analysis. The analysis is carried out for the applied fatigue load cycle ($R_p = 0$) using Paris law with Elber correction model as described in Sect. 3.4. The maximum load in the fatigue cycle is taken as 75% of the failure load computed for the adhesively bonded joint without damage considering the typical design criteria of aircraft components. The crack which is away from support edges ($\lambda/L = 0.875$) and near to discontinuities to the support conditions (Fig. 11). Further, the crack propagation within the overlap region for the applied fatigue load cycles is much slower compared to the cracks away from the overlap region due to additional stiffness and less bending effects. In addition, when a crack of size ‘ v ’ is detected at the location, $\lambda/L = 0.75$, the remaining cycles to reach the critical crack length (residual life) have been determined and are shown in Fig. 11. Similar exercise can be carried out for other crack locations and sizes.

Fig. 8 Variation in SIF along the depth of the adherent plate

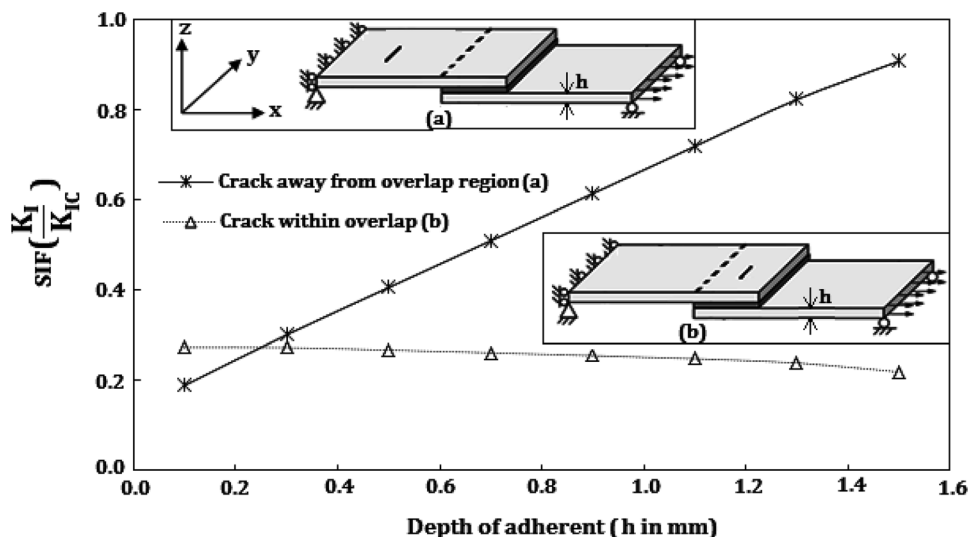


Fig. 9 SIF variation for the cracks in adherent away from overlap region

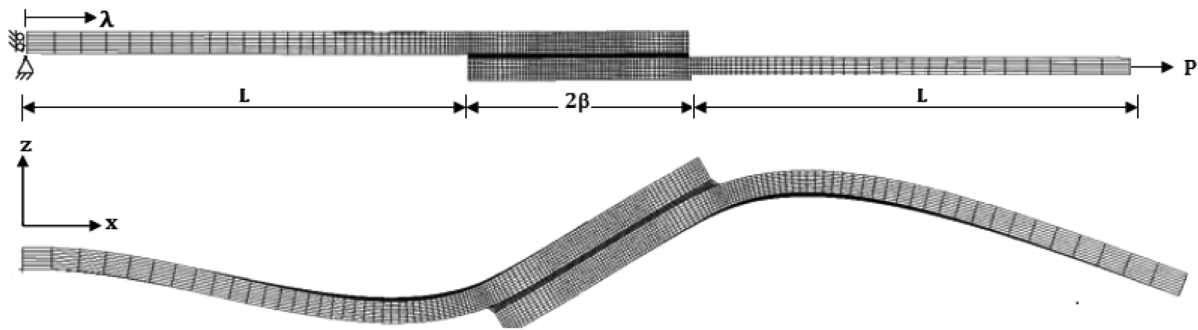
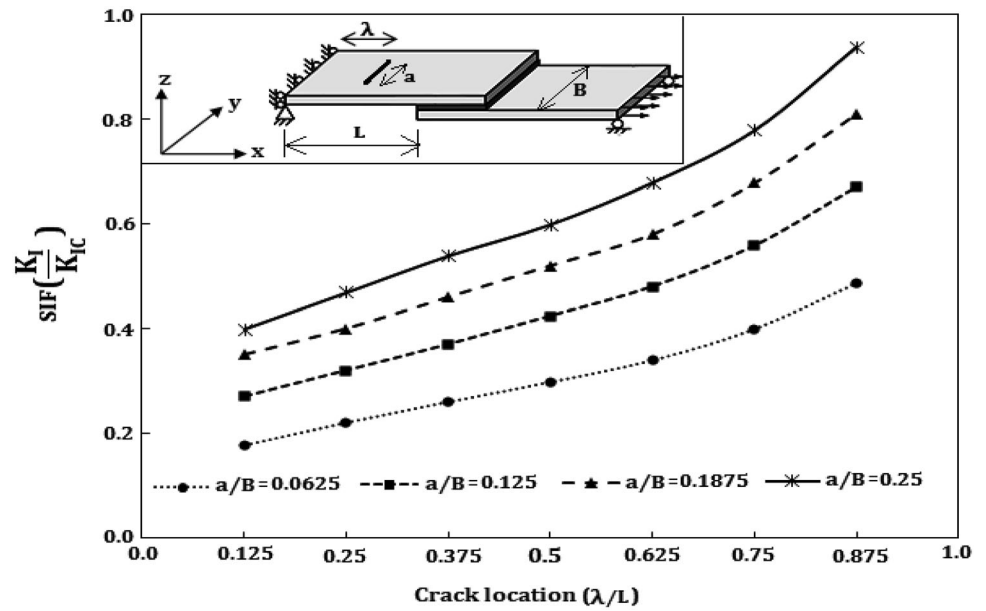
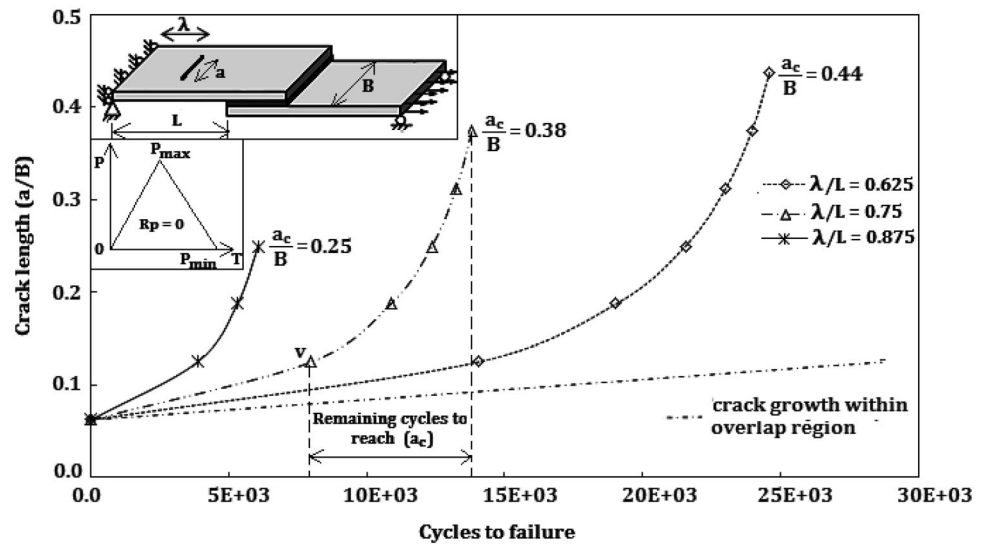


Fig. 10 Deformation of adhesively bonded single-lap joint when subjected to axial load

Fig. 11 Crack propagation in adherent plate



Summary and conclusions

- Three-dimensional finite-element analysis of adhesively bonded single-lap joints is conducted using MSC PATRAN and MSC NASTRAN with eight-node brick elements considering material and geometric nonlinearity effects.
- The peel and shear stresses from the current analysis are validated with the results from the literature.
- Failure load of these joints in the absence of damage is calculated using average stress criterion utilizing ‘characteristic distance’ concept in the overlap region.
- Further, small allowable initial crack length is assumed at different locations in the adherent plates and fracture parameters are computed by MVCCI technique. While SIF increases along the thickness from top to bottom for the crack in the adherent plate away from overlap region, there is no significant depthwise SIF variation for crack within the overlap region.
- The adherent plates with crack away from the overlap region show a tendency towards failure at lower loads than the cracks in the overlap region. This behaviour is typically exploited for designing the repair of damages in thin-walled structures using adhesively bonded patch that provides alternative load paths, thus retarding the crack growth.
- Among the cracks outside the overlap region, crack which is farther from the support condition is more prone to failure due to bending effects.
- This prognostic approach in estimating the remaining life of adhesively bonded joints in the presence of damage may aid for better SHM-based design.

References

- Adams RD, Peppiatt NA (1974) Stress analysis of adhesive-bonded lap joints. *J Strain Anal* 9(3):185–196
- Badari Narayana K, Dattaguru B, Ramamurthy TS, Vijaykumar K (1994) A general procedure for modified crack closure integral in 3D problems with cracks. *Eng Fract Mech* 8(2):167–176
- Bharath K, Chikmath L (2017) Prognosis analysis of tapered attachment lugs with interference and clearance fits under fatigue loading. *ISSS J Micro Smart Syst* 6(1):15–28
- Chun HW, Peter C (2000) Plastic yielding of a film adhesive under multiaxial stresses. *Int J Adhes Adhes* 20(2):155–164
- Clark JD, McGregor IJ (1993) Ultimate tensile stress over a zone: a new failure criterion for adhesive joints. *J Adhes* 42(4):227–245
- Dattaguru B, Everett RA Jr, Whitcomb JD, Johnson WS (1984) Geometrically nonlinear analysis of adhesively bonded joints. *J Eng Mater Technol* 106(1):59–65
- Elber W (1971) The significance of fatigue crack closure. In: Rosenfeld M (ed) *Damage tolerance in aircraft structure*, vol 486. ASTM, Philadelphia, pp 230–242
- Gomez MP, Ernst H, Vazquez J (1976) On the validity of Elber’s results on fatigue crack closure for 2024-T3 aluminium. *Int J Fract* 12:178–180
- Gopalan R (1991) A study on hygrothermal effects on advanced composites and adhesively bonded joints. Ph.D. thesis Department of Aerospace Engineering, Indian Institute of Science, Bengaluru, India
- Haapalainen J, Leskela E (2012) Probability of detection simulations for ultrasonic pulse-echo testing. In: *18th World conference on non-destructive testing, Durban-South Africa*, pp 16–20
- Hart-Smith LJ (1973) Adhesive-bonded single-lap joints. NASA technical report, Langley research centre-USA, CR 112236
- Jamal-Omidi M, Mohammadi SMR (2018) Investigation of defect effects on adhesively bonded joint strength using cohesive zone modelling. *J Mech Eng* 68(3):5–24
- Karachalios EF, Adams RD, da Silva Lucas FM (2013) Strength of single lap joints with artificial defects. *Int J Adhes Adhes* 45:69–76
- Kinloch JA, Osiyemi SO (1993) Predicting the fatigue life of adhesively-bonded joints. *J Adhes* 43(1–2):79–90
- Kumar U, Kumar P, Noor MT, Das RR (2018) FEM based delamination damage analysis of bonded FRP composite pipe joints. *ISSS J Micro Smart Syst* 7:45–51
- Mortensen F, Thomsen OT (2002) Analysis of adhesive bonded joints: a unified approach. *Compos Sci Technol* 62(7–8):1011–1031
- Pandey PC, Narasimhan S (2001) Three-dimensional nonlinear analysis of adhesively bonded lap joints considering viscoplasticity in adhesives. *Comput Struct* 79(7):769–783
- Philip WY, Craig SC, Brett AB (2006) Failure analysis of adhesively bonded composite joints via the virtual crack closure technique. In: *47th AIAA structures, structural dynamics and materials conference*, Newport Island, USA
- Sahoo PK, Dattaguru B, Manjunatha CM, Murthy CRL (2012) Fatigue de-bond growth in adhesively bonded single lap joint. *Sadhana* 37(1):79–88
- Sargent JP (2005) Durability studies for aerospace applications using peel and wedge tests. *Int J Adhes Adhes* 25(3):247–256
- Shanley F (1943) Aircraft structural research. *Aircr Eng Aerosp Technol* 15(7):200–206
- Struck H (1977) Factor of safety/limit load concept-maximum load concept. AGARD Rep 661:1–14
- The MSC NASTRAN documentation (2017) MSC Software Corporation, Macarthur Court, Newport Beach-CA, USA, 4675
- The MSC PATRAN documentation (2017) MSC Software Corporation, Macarthur Court, Newport Beach-CA, USA, 4675
- Tsai MY, Morton J (1994) An evaluation of analytical and numerical solutions to the single-lap joint. *Int J Solids Struct* 31(18):2537–2563
- Vivek M (2007) A conceptual aerospace structural system modelling, analysis and design process. In: *48th AIAA structures, structural dynamics and materials conference*, Honolulu, USA

Publisher’s Note Springer Nature remains neutral with regard to jurisdictional claims in published maps and institutional affiliations.